A Macrothermodynamical Approach to the Limit of Reversible Capillary Condensation

Philippe Trens, **Nathalie Tanchoux**, **Francesco Di Renzo**, **François Fajula**

Laboratoire des Matériaux Catalytiques et catalyse en Chimie Organique, Ecole Nationale Supérieure de Chimie de Montpellier, FR 1878 Institut Gerhardt, 8 rue de l'Ecole Normale, 34296, Montpellier Cedex 5, France

Extended abstract

A hysteresis loop is such a common occurrence in the adsorption-desorption cycles on mesoporous adsorbents that its presence has been included in the IUPAC definition of the type IV isotherm. It was early observed that no hysteresis loop can extend below a given relative pressure threshold, p/p° = 0.42 in the case of N2 at 77 K. Any desorption loop begun at higher pressure is terminated by a sudden evaporation when this threshold of relative pressure is reached. This effect, suggestively defined as catastrophic desorption, is at the basis of a frequent artefact in the evaluation of pore size: the sudden desorption is attributed to a narrow distribution of pores around 4 nm diameter, albeit the actual porosity has smaller size and is more broadly distributed. For smaller mesopores, in which capillary condensation takes place below the lowest possible closure point of the hysteresis loop, pores are filled and emptied following the same reversible path. For each pore size and shape, the pressure of the hysteresis closure point depends both on the nature of the adsorbate and on the temperature. The absence of hysteresis in the adsorption-desorption cycle for small mesopores was attributed to a tensional instability of the meniscus at low curvature radius. The smaller the mesopores are, the larger the capillary tension experienced by the liquid is. For very small mesopores, the tension can exceed the tensile strength of the liquid, which cannot help to evaporate. Conditions in which a liquid-gas interface is unstable are strongly reminiscent of the definition of the critical point of a fluid. Since the beginning of the eighties, a large research effort has been devoted to the evaluation of the critical properties of confined fluids. NLDFT calculations allowed simulating the adsorption and desorption branches of the isotherm in porous systems. It was calculated that a mesopore is filled and emptied along the same path above a threshold of temperature and pressure defined as a capillary critical point.

The threshold of reversible capillary condensation is a well-defined thermodynamical property, as evidenced by corresponding states treatment of literature and experimental data on the lowest closure point of the hysteresis loop in capillary condensation-evaporation cycles for several adsorbates.

Experimental section.

Sample preparation and textural characterization. MCM-41 type silica adsorbents were used in this work. These were prepared in the presence of either hexadecyl trimethyl ammonium cations (25Å MCM-41) in some cases accompanied by a swelling agent as hexadecyl dimethyl amine (44Å MCM-41) or trimethylbenzene (84Å MCM-41 and 95Å MCM-41). The textural specifications of the materials, as evaluated by nitrogen adsorption at 77 K, are summarized in table 1.

Table 1. Specific surface area, mean pore size and mesopore volume of the adsorbents measured by N_2 adsorption at 77K. The cross sectional area of nitrogen has been taken as 0.162 nm^2.

Sample	S_{BET} / $m^2.g^{-1}$	D_p / nm	V_p / $cm^3.g^{-1}$
2.5 MCM-41	965	2.5	0.73
4.4 MCM-41	1180	4.4	1.11
8.4 MCM-41	924	8.4	1.99
9.5 MCM-41	854	9.5	1.99

The condensing mixture was heated in an autoclave reactor at 393 K for 2 days. The template was then removed by calcination under air flow ($30cm^3.min^{-1}$) at 823 K for 5 hours to generate the mesoporosity. The temperature ramp was 1 $K.min^{-1}$. The final material was characterized by nitrogen adsorption at 77K and powder X-ray diffraction (not presented here). Nitrogen adsorption at 77 K on the MCM-41 material gives a type IV adsorption isotherm, with a steep capillary condensation uptake and a well defined saturation plateau,

typical of highly ordered mesoporous materials. The XRD pattern exhibits three reflections, which can be indexed according to a hexagonal (P6mm) structure. The [100] reflection (narrow, well defined) allowed to derive a distance between one pore wall to an equivalent position in the adjacent wall of *ca.*3.9 nm. The synthesized material is characterized by a specific surface area of *ca* 1200 $m^2.g^{-1}$, a pore diameter of 3.6 nm, and a pore volume of 0.95 $mL.g^{-1}$.

Adsorption studies. Sorption isotherms were determined using a home-built volumetric adsorption apparatus described elsewhere.[1] N-hexane (Aldrich, Purity >99.9%) and 1-hexene (Aldrich, Purity >99%) were outgassed prior to use by freezing-thaw cycles under primary vacuum. 150 mg of the mesoporous material were used for the adsorption experiments in the range of temperature 273 - 333 K. The equilibrium time for each experimental data point ranged between 30 min. and 120 min. depending on its location on the sorption curve.

To our data concerning the adsorption of n-hexane and 1-hexene but also nitrogen and oxygen, extra sorption isotherms were also collected from the literature. All materials used in the cited studies are mesoporous materials and they have a mean pore diameter of 3.6 nm (which may slightly vary, depending on the model used for the pore diameter determination) and the adsorbates used in those studies were either gases or vapours (argon[, 2], xenon[3], oxygen[4, 5], 2,2-dimethylbutane[3], cyclopentane[Erreur ! Signet non défini.] or benzene[3]).

Results and Discussion.

Adsorption isotherms.

The influence of temperature and pore size over the adsorption of n-hexane or 1-hexene on the MCM-41 material is reported in figures 1 and 2.

In figure 1, it can be seen that the adsorption isotherms belong to the type IV according to the IUPAC classification: the curves exhibit a slight knee at low relative pressure (in the case of n-hexane, the adsorption curves almost follow a straight line which indicates its poor affinity for silica surfaces), followed by a steep capillary condensation step and a clear

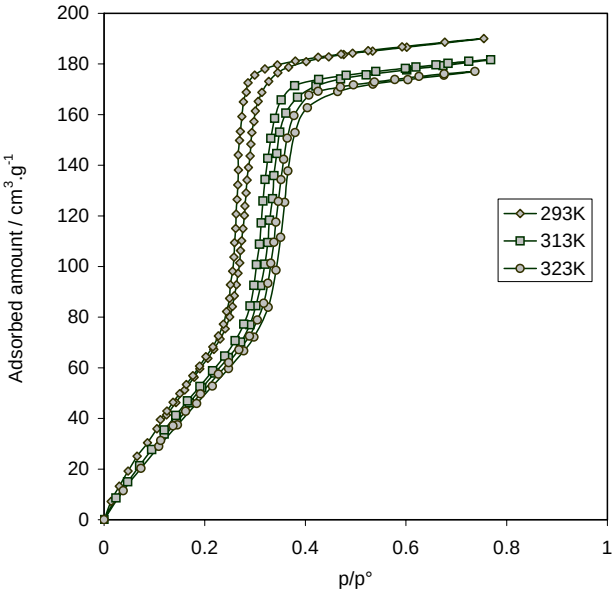

Figure 1. Adsorption isotherms of n-hexane over 4.4 MCM-41 at different temperatures.

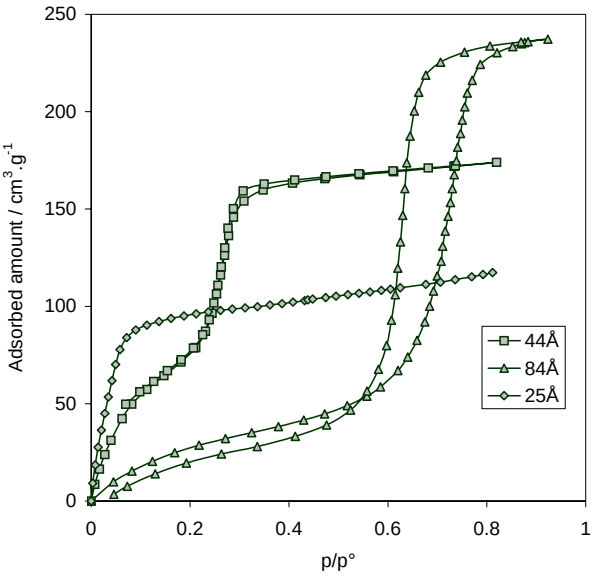

Figure 2. Adsorption isotherms of 1-hexene at 293 K over different pore sizes MCM-41.

saturation plateau. The steepness of the capillary condensation indicates a very narrow pore size distribution (which is directly predicted by the Kelvin equation), confirming the high order suggested by the XRD diffractogram. The low uptakes observed during the adsorption on the saturation plateaus shows that the material used is essentially mesoporous with a very small extent of external surface. As expected, saturation plateaus shift to low adsorbed amounts as temperature increase, due to the variation of density of sorbates for the different temperatures examined. The adsorption isotherms of n-hexane exhibit a hysteresis loop which shifts towards high relative pressure as temperature increases as already found for other systems, experimentally or by simulation theories. [67] In figure 2, the influence of pore size can be demonstrated: for a given temperature, (here 293 K) the hysteresis loop appears as pore size increases as usually found in the literature. [8910]

Further, it can be noted that the adsorption isotherm corresponding to the small pore size material (2.5 MCM-41) is no longer of the type IV adsorption isotherm, but more probably between types I and IV, typically between microporous and mesoporous adsorption processes as it can be also deduced from the ratio pore diameter / kinetic molecular diameter (around 5).

Energetics of capillary condensation processes.

The energetic parameters accompanying the adsorption processes have been derived using the isosteric method in the case of the different pore size materials. The differential enthalpy of adsorption can be derived (according to eq. 5) from a set of adsorption isotherms provided that the temperature range in which the different curves have been determined is not too large.

$$\Delta_{ads} h \quad = \quad -RT^2 \times \left[\frac{\partial(\ln\, p)}{\partial T} \right]_{\Gamma} \tag{1}$$

A mean value of the enthalpy of condensation of n-hexane and 1-hexene in the mesopores could be derived and are reported hereafter in table 2 where are also reported the enthalpies of condensation of the free (unconfined) vapours. As already published in the literature, [11-12] it can be noted that the differential enthalpies of condensation in confined environments are higher than those corresponding to the free vapours. This can be interpreted in terms of scaling effects. [13] The final equation describing this phenomenon has already been developed and clarified and it can be written as follows (eq. 2):

$$\Delta h_{filling} = \Delta h_{cond} - \frac{N_m \times \Delta h_{interface}}{N_{filling}} \times \sqrt{\frac{V_{filling}}{V_{pore}}} \tag{2}$$

where $\Delta h_{filling}$ is the latent enthalpy of condensation during pore filling, Δh_{cond} is the latent enthalpy of condensation in the bulk, N_m, the monolayer capacity, $\Delta h_{interface}$, the enthalpy of formation of the liquid/gas interface, $N_{filling}$, the amount of gas condensing in the mesopores, $V_{filling}$, the volume of gas condensing in the mesopores and V_{pore} the total pore volume.

Δh_{cond} can be found from the literature, [39] N_m can be estimated from the BET transform of adsorption isotherms. $\Delta h_{interface}$, has been estimated from the surface tension of 1-hexene at 303 K (0.020 $mJ.m^{-2}$) and the monolayer capacity at the same temperature; a value of 12.90 $kJ.mol^{-1}$ has been found. $N_{filling}$, $V_{filling}$ and V_{pore} can be estimated from the adsorption isotherms. The comparison between the isosteric heats of condensation and the results yielded by using our model are reported, figure 3.

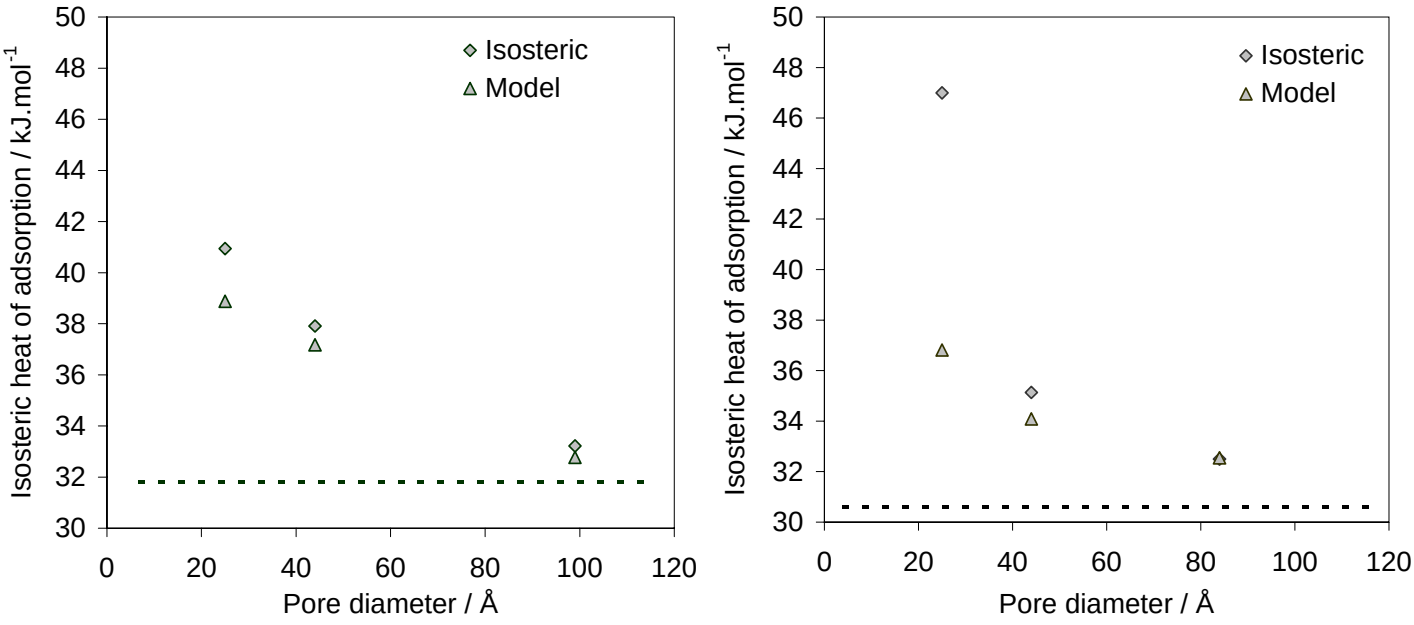

Figure 3. Comparison between heat of condensation and the results obtained using our model (left n-hexane, right, 1-hexene).

The model perfectly fits the results in the case of n-hexane: enthalpic excesses are well described even in the case of small pore size MCM-41. The same agreement can be observed for the adsorption of 1-hexene, even though a large discrepancy can be observed in the case of the small pore size material. This is probably due to the fact that the adsorbing system is at the border between microporous and mesoporous systems, thus interfering between multilayer adsorption and capillary condensation.

Table 2. Comparison between the differential enthalpies of condensation in the mesopores and the differential enthalpies of condensation of the free (unconfined) vapours.

Pore size	n-hexane Δh / -kJ.mol^{-1}	1-hexene Δh / -kJ.mol^{-1}
Free vapour	31.56	30.60
2.5 nm	40.94	47.00
4.4 nm	37.91	35.14
8.4 nm	-	32.50
9.5 nm	33.22	--

Comparison between adsorbing systems.

For our experimental systems and also for other systems taken from the literature, a comparison between the different adsorption-desorption isotherms on different systems can be made. Thus, a value of pressure p and temperature T can be extracted either as the lowest closure point of the hysteresis loop of each sorption isotherm if any, or as the inflexion point of the capillary condensation uptake when the sorption curve was fully reversible.

The principle of corresponding states has been used to evaluate the differences between systems at the lowest point of the hysteresis loops. This principle can be summarized by saying that gases at the same volume and temperature exert the same reduced pressure. [14] A reduced variable is obtained by dividing a real variable by its corresponding critical value. When plotting the same data in this new set of reduced variables, figure 3 is obtained, by using a Clausius Clapeyron formalism.

When plotting $Ln(p_R)$ versus $1/T_R$, straight lines are obtained. However, the relative position of the curves on the graph clearly appears to depend on the nature of the adsorbate (vapors higher than gases), which is apparently in contradiction with the principle of corresponding states because one would expect that all data lie on the same curve.

However, it is well known that this principle works best for gases composed of spherical molecules but it fails when the molecules are polar or non-spherical which is the case here, for the organic vapors and some gases.

We used acentric factors ω, first developed by Pitzer, taking into account the non-sphericity of molecules and therefore their polarisability as a contribution for the non-ideality of real gases. [15-16] Acentric factors have been defined as: $\omega = -\log_{10} P_{vp,r}\big|_{T_r=0.7} - 1$ because the monoatomic gases (Ar, Kr and Xe) have ω ~ 0 and except for quantum gases (H_2, He or Ne), all other species have positive values up to 1.5. To obtain values of acentric factors ω, one needs the constants p_c, T_c and the value of vapor pressure at the reduced temperature $T/T_c = 0.7$. The reciprocal of T/T_c is the X-axis of figure 4 and the values of ω can be read for $1/T_R = 1.42$.

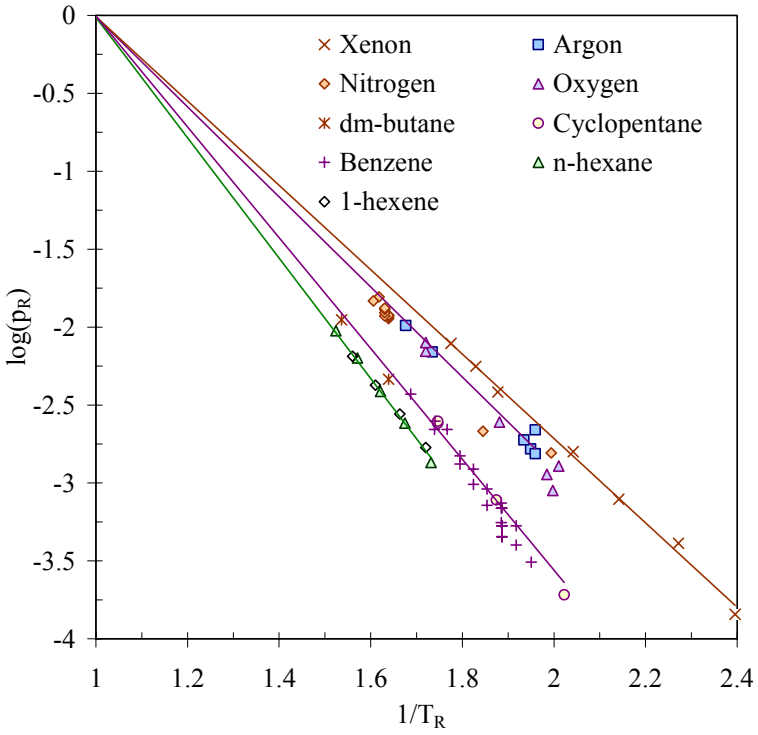

Figure 4. Limits of reversibility of adsorption isotherms plotted for different systems in a Clausius Clapeyron formalism in reduced coordinates.

The non-hysteretical filling of small mesopores presents the properties of a first-order phase transition, confirming that the condensation reversibility does not depend on the capillary shift of the critical point. The enthalpy of reversible capillary condensation can be calculated by a Clausius- Clapeyron approach and is consistently larger than the condensation heat in unconfined conditions. The limit of reversible pore filling (rpf limit) has been empirically defined as the relative pressure level below which adsorption and desorption in a mesoporous system follow the same path. The attempts to identify the rpf limit with the critical point of

the confined fluid have failed. Nevertheless, the rpf limit can be defined on the basis of macro-thermodynamical properties. Its dependence on temperature follows corresponding

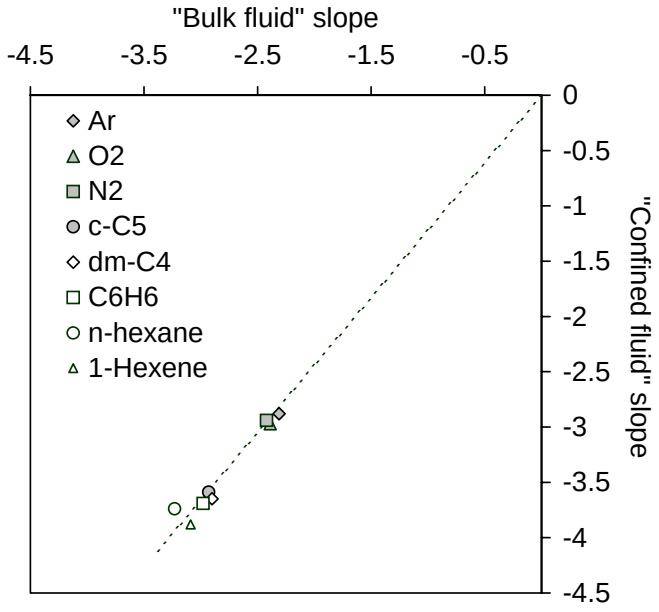

Figure 5. Vapour liquid phases transitiion versus limit of reversibility of adsorption isotherms

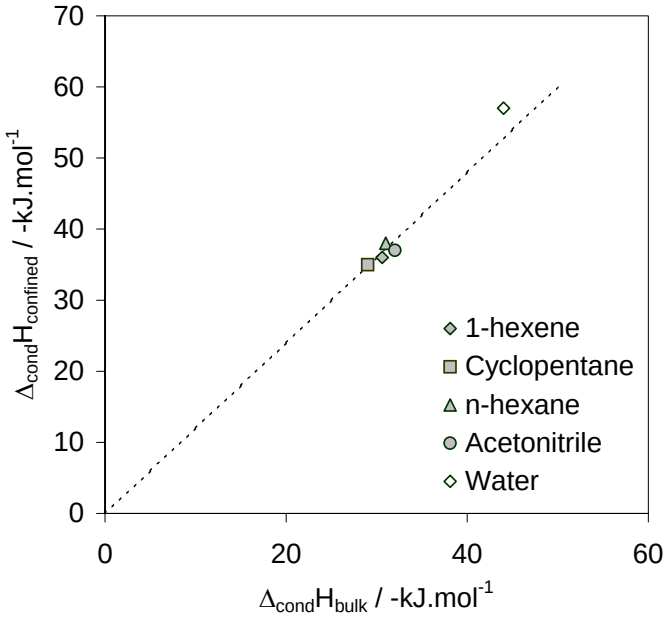

Figure 6. Differential enthalpies of condensation in the mesopores versus differential enthalpy of free vapours

states relations and strongly suggests that it has to be considered as a first-order gas-liquid transition in the confined environment of the mesopores. The data on which this paper is drawn seem quite general, applying to adsorbates as different as argon and benzene. The nature of the adsorbent seems not to be a determining factor, experimental data on several adsorbents (silica, zirconia, magnesia, and carbon) having been used. An important property of the rpf limit is a value of transition enthalpy significantly higher than the condensation enthalpy on a flat liquid surface. It seems to correspond to a given threshold in the continuous evolution of adsorption enthalpy with confinement (figures 5 and 6). The rpf limit can likely be defined as the threshold of confinement beyond which the properties of the adsorbed layer create an infinite probability of formation of bridges between the layers adsorbed on the opposite walls of the pore. In this way, adsorption behaves no more as an activated process and is superposed to the equilibrium desorption curve. It is also significant that a

macrothermodynamical treatment can provide useful information on the condensation in pores not larger than 10 molecular sizes, a domain usually reserved to statistical thermodynamics. This enthalpic advantage makes easier the overcoming of the adhesion forces by the capillary forces and justify the disappearing of the hysteresis loop.

References

(1) Tanchoux, N.; Trens, P.; Maldonado, D.; Di Renzo, F.; Fajula, F. *Colloids Surf.* **2004**, *246*, 1.

(2) Llewellyn, P.L.; Schüth, F.; Grillet, Y.; Rouquerol, F.; Rouquerol, J.; Unger, K. K. *Langmuir* **1995**, *11*, 574.

(3) Machin, W.D.; Golding, P.D. *J.Chem.Soc.Farad.Trans.* **1990**, *86*, 171.

(4) R.M. Barrer, D.M. MacLeod, *Trans. Faraday Soc.* **1954**, *50*, 980

(5) R.M. Barrer, N. McKenzie, J.S.S. Reay, *J. Colloid Sci.* **1956**, *11*, 479.

(6) Franke, O.; Schulz-Ekloff, G.; Rathousky, J.; Starek, J.; Zukal, A. *J. Chem. Soc. Chem. Commun.* **1993**, 724.

(7) Branton, P. J.; Hall, P. G.; Sing, K. S. W.; Reichert, H.; Schüth, F.; Unger, K. K. *J. Chem. Soc. Faraday Trans.* **1994**, *90*, 2965.

(8) Ravikovitch, P. I.; Domhnaill, S. C. O.; Neimark, A. V.; Schüth, F.; Unger, K. K. *Langmuir* **1995**, *11*, 4765.

(9) Morishige, K.; Shikimi, M. *J. Chem. Phys.* **1998**, *108*, 7821.

(10) Qiao, S.Z.; Bathia, S. K.; Nicholson, D. *Langmuir* **2004**, *20*, 389.

(11) A. V. Neimark, P. I. Ravikovitch, M. Grun, F. Schuth, K. K. Unger, J. Colloid Interf. Sci. 207(1) (1998) 159.

(12) P. Trens, N. Tanchoux, D. Maldonado, P. M. Papineschi, F. Di Renzo, F. Fajula, Microp. Mesop. Mater. **2005**, 86, 354-363.

(13) P. Trens, N. Tanchoux, D. Maldonado, A. Galarneau, F. Di Renzo, F. Fajula, New J. Chem. 28 (2004) 874-879.

(14) Guggenheim, E. A. *J. Chem. Phys.* **1945**, *13*, 253.

(15) Pitzer, K. S.; Curl, R. F. *J. Am. Chem. Soc.* **1955**, *77*, 3427.

(16) Reid, R. C.; Prausnitz, J. M.; Sherwood, T. K. in *The properties of gases and liquids*, 3rd edition; Mc Graw-Hill Ed.: New York, United States, 1976.